Materials Physics and Mechanics 47 (2021) 727-738
Research article

Received: September 22, 2021
Accepted: November 5, 2021

EXPERIMENTAL STUDY AND MODELING OF CHANGING MECHANICAL PROPERTIES IN TEMPERING OF BAINITIC-MARTENSITIC STEELS

A.A. Vasilyev[1]✉, D.F. Sokolov[2], S.F. Sokolov[2]

[1]Peter the Great St. Petersburg Polytechnic University, Polytekhnicheskaya, 29, 195251, St. Petersburg, Russia

[2]PJSC Severstal, Mira, 30, 162608, Cherepovets, Russia

✉ vasilyev_aa@mail.ru

Abstract. Dependences of mechanical properties (yield stress, tensile stress, relative elongation) and impact toughness on the tempering time at various temperatures have been investigated for 10 industrial bainitic-martensitic steels with a wide range of chemical compositions (C(0.04-0.27), Mn(0.33-1.57), Si(0.22-1.09), Cr(0.02-1.14), Ni(0.01-3.74), Cu(0.02-1.03), Mo(0.01-0.43), Nb(0.002-0.044), V(0.003-0.200), Ti(0.001-0.045), B(≤0.003) (mass.%)). Based on the obtained experimental results, a quantitative model is developed to predict the mechanical properties of the considered steels after tempering. The modeling results comply well with experiments. The average relative errors in predicting the yield and tensile stresses are, respectively, 5.9 and 5.3%, and the average absolute error in predicting the relative elongation is 2.5%.

Keywords: steels, tempering, microstructure, mechanical properties, modeling

Acknowledgments. *Grant from the Russian Science Foundation (project No. 19-19-00281).*

Citation: Vasilyev A.A., Sokolov D.F., Sokolov S.F. Experimental study and modeling of changing mechanical properties in tempering of bainitic-martensitic steels // Materials Physics and Mechanics. 2021, V. 47. N. 5. P. 727-738. DOI: 10.18149/MPM.4752021_7.

1. Introduction

Mechanical properties of quenched bainitic-martensitic steels significantly depend on their following tempering. Accordingly, a lot of works are aimed to investigate and simulate complex multi-stage precipitation processes of various type particles in tempering [1-5] as well as their effects on final steel properties. The authors have described a model [5] for the tempering effects on quenched Cr-Mo-V-Cu bainitic-martensitic steels that allows for both the recovery and precipitation phenomena. The latter involves various carbides (Fe_3C, V_4C_3, Mo_2C, Cr_7C_3) and particles of pure Cu. However, to get desired mechanical properties of the considered materials, quantitative models to predict these properties are additionally required.

The present paper represents experimental results on the dependences of mechanical properties and impact toughness on the tempering time at various temperatures as obtained on 10 industrial steels with a wide range of chemical compositions. Based on these data, a quantitative model is described to predict the mechanical properties of the considered steels after tempering. Apart from the obtained experimental results, the model calibration also has employed microstructural parameters derived by means of the AusEvol Pro software [6,7]

http://dx.doi.org/10.18149/MPM.4752021_7

using data on the industrial mode of hot rolling, subsequent cooling, and quenching of steel plates in a roller-quenching machine.

2. Investigated steels, experimental procedures, and results

Dependences of mechanical properties (yield stress, ultimate tensile stress, relative and impact toughness on the tempering time at various temperatures have been investigated 10 industrial bainitic-martensitic steels with a wide range of chemical compositions (C(0.04-0.27), Mn(0.33-1.57), Si(0.22-1.09), Cr(0.02-1.14), Ni(0.01-3.74), Cu(0.02-1.03), Mo(0.01-0.43), Nb(0.002-0.044), V(0.003-0.200), Ti(0.001-0.045), B(≤0.003)) listed in Table 1.

Table 1. Chemical compositions of the investigated steels (mass.%)

Steel	C	Mn	Si	Cr	Ni	Cu	Mo	Nb	V	Ti	B
S1	0.21	0.56	0.25	0.75	0.10	0.14	0.02	0.002	0.003	0.002	–
S2	0.12	0.45	0.25	0.59	0.06	0.12	–	0.024	0.053	0.003	–
S3	0.10	1.56	0.29	0.12	0.13	0.13	0.01	0.044	0.066	0.005	–
S4	0.10	0.34	0.22	0.41	1.91	0.52	0.26	0.003	0.032	0.002	–
S5	0.11	0.54	0.85	0.75	0.66	0.42	0.02	0.002	0.005	0.005	–
S6	0.27	0.58	1.09	0.85	1.42	0.06	0.23	0.023	0.007	0.045	0.003
S7	0.10	1.57	0.27	0.02	0.01	0.02	–	0.036	0.039	0.014	–
S8	0.12	1.01	0.24	1.14	0.19	0.17	0.41	0.031	0.005	0.003	0.002
S9	0.12	0.55	0.27	1.10	0.10	0.10	0.30	0.004	0.200	0.003	–
S10	0.04	0.33	0.26	0.65	3.74	1.03	0.43	0.002	0.142	0.001	0.001

Samples of 45×450 mm section were cut from hot rolled plates of 9÷16 mm thickness cooled in the roller-quenching machine of PJSC "Severstal". The samples have been tempered in laboratory furnace Nabertherm (model N60/65HA) at temperatures 400, 500, 600, and 650°C; 8 holding times (0.5, 1, 1.5, 2, 3, 4, 5, 6 h) have been used at each of these temperatures. Specimens have been made for both the quenched and tempered states.

Tensile tests according to GOST 1497-84 are implemented on industrial machines of PJSC "Severstal", and the impact toughness (KCV) are determined according to GOST 9454-78 by means of installment Zwick/Roell RKP-450. Quenched structures are analyzed with optical microscope Axio Observer "Carl Zeiss".

Micrographs of quenched steel structures are shown in Fig. 1 whereas their characteristics are represented in Table 2 that also lists theoretical volume fractions of various structural constituents as derived by means of AusEvol Pro software [6,7] from given industrial modes of hot rolling and following cooling conditions. According to these data, calculation results comply well with images of the considered structures of mostly bainitic-martensitic type. Some deviations are due to difficulty in the visual estimate of low fractions peculiar to polygonal ferrite and granular bainite as well as to the complicated discrimination between martensite and lath bainite.

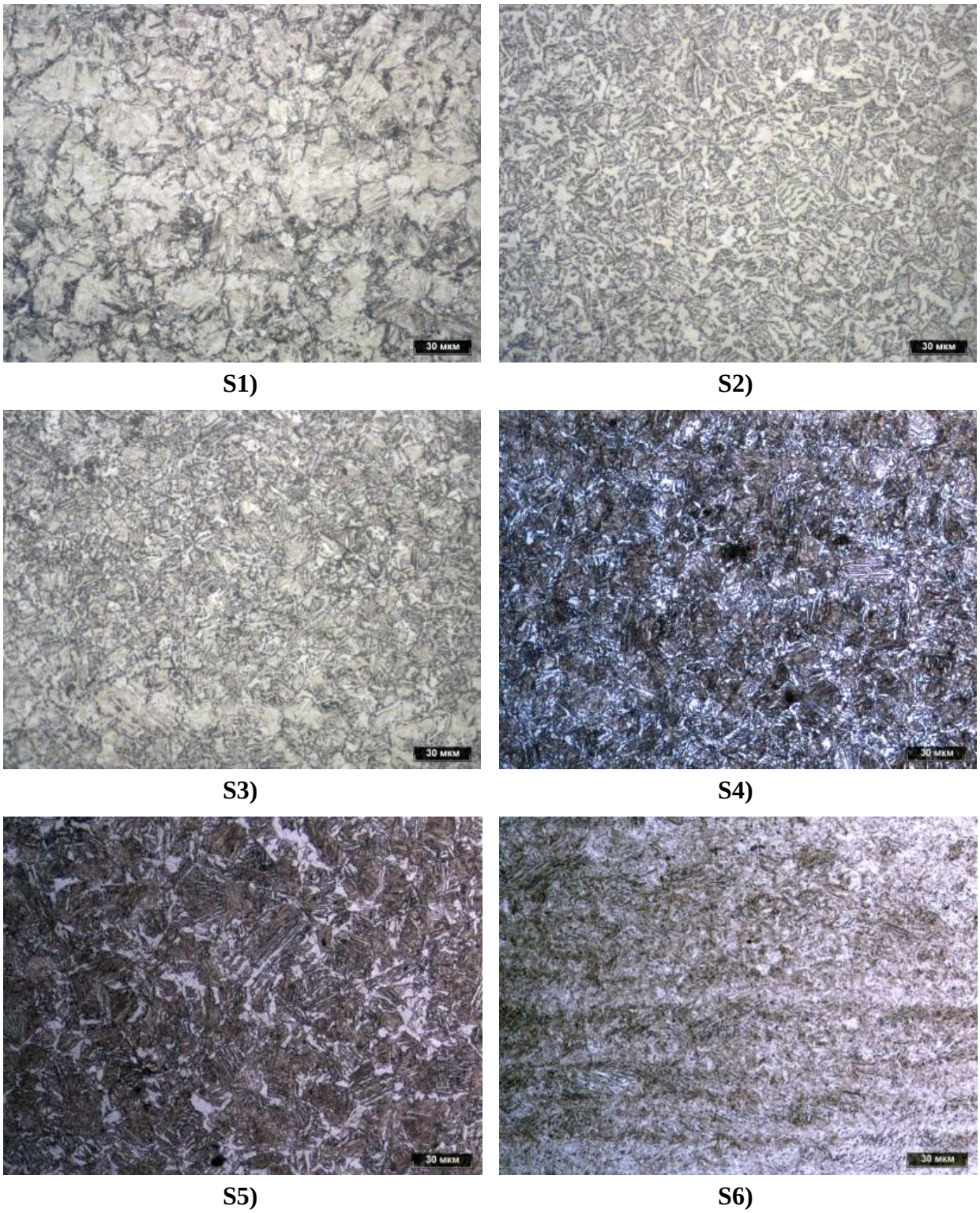

Fig. 1. Optical images (×500) of microstructures of the studied steels after quenching (S1-S6)

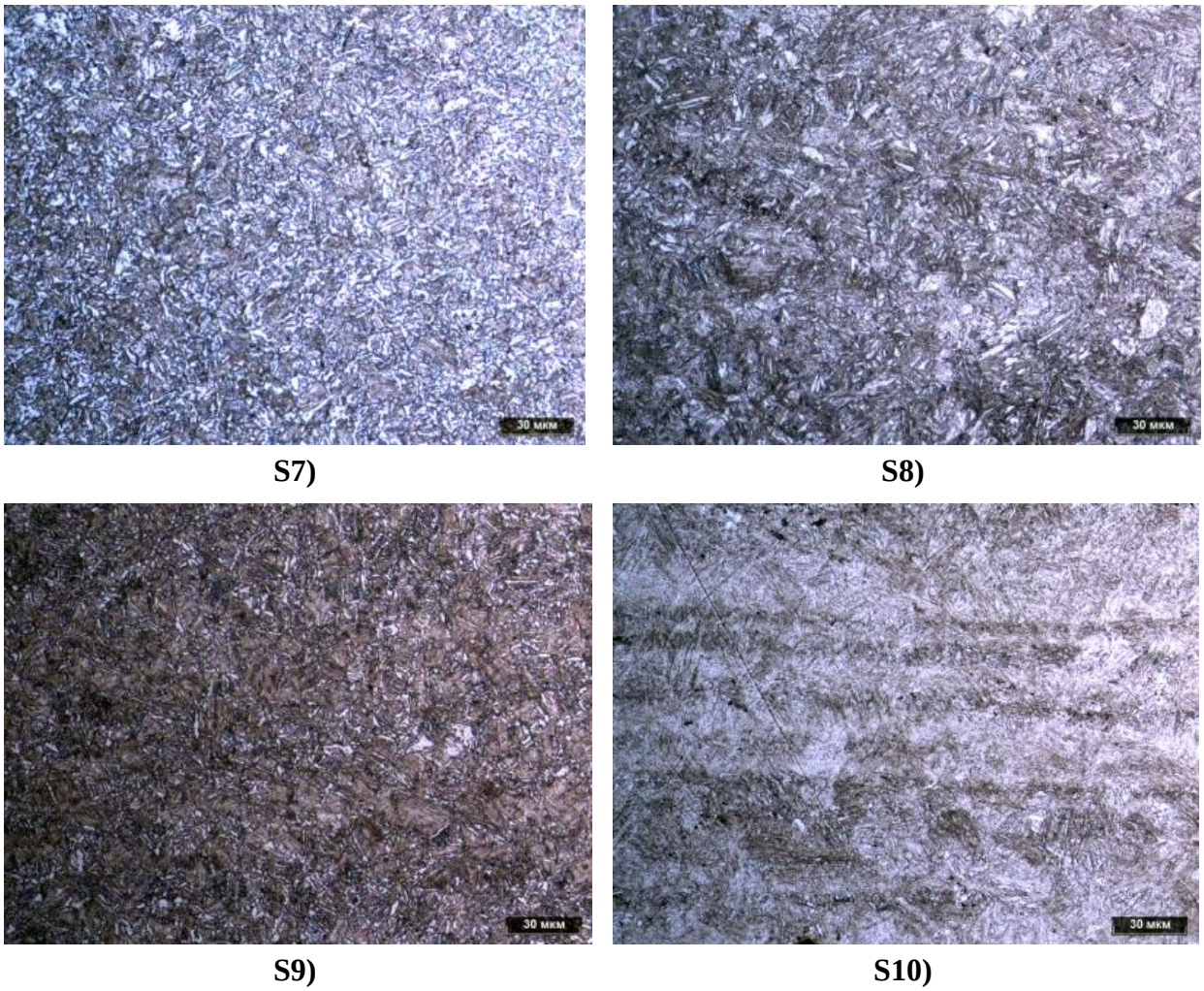

S7) **S8)**

S9) **S10)**

Fig. 1. Optical images (×500) of microstructures of the studied steels after quenching(S7-S10)

Table 2. Characteristics of steel microstructures after quenching

Steel	Type of the microstructure	
	Visual estimation	Calculated volume fractions of the components, %
S1	PF↓ + LB + M	3PF + 25LB + 72M
S2	PF↓ + GB + LB	8PF + 58GB + 34LB
S3	GB + LB + M	52ГБ + 36РБ + 12М
S4	PF↓ + LB + M	5PF + 1GB + 76LB + 18M
S5	PF↓ + LB + M	2PF + 5GB + 62LB + 31M
S6	LB + M	20LB + 80M
S7	PF↓ + GB + LB	11GB + 89LB
S8	LB + M	2GB + 22LB + 76M
S9	LB + M	1GB + 56LB + 43M
S10	M	46LB + 54M

*PF – polygonal ferrite (↓ − low fraction); GB – granular bainite; LB – lath bainite; M – martensite

Mechanical properties and the impact toughness of some from the investigated steels are represented in Fig. 2.

a)

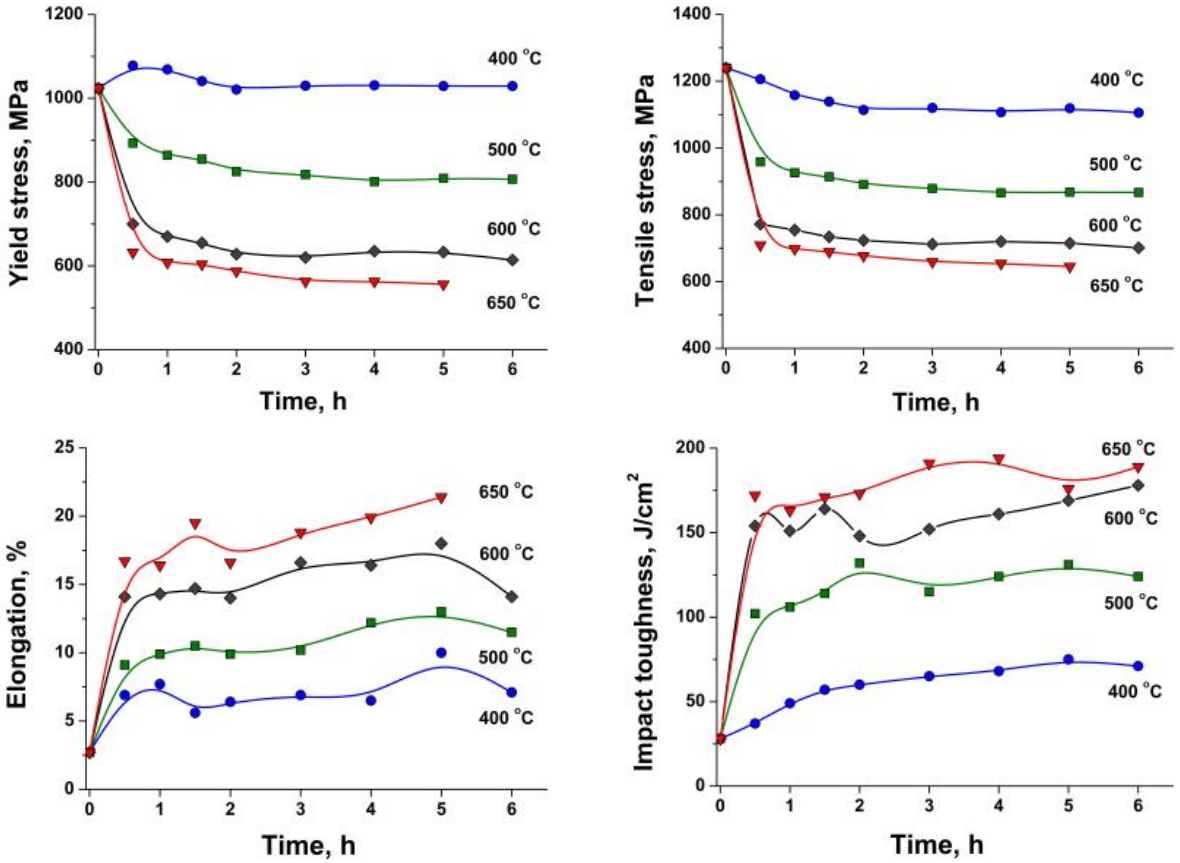
Yield stress, MPa
Time, h
400 °C
500 °C
600 °C
650 °C
Tensile stress, MPa
Time, h
Elongation, %
Time, h
Impact toughness, J/cm²
Time, h

b)

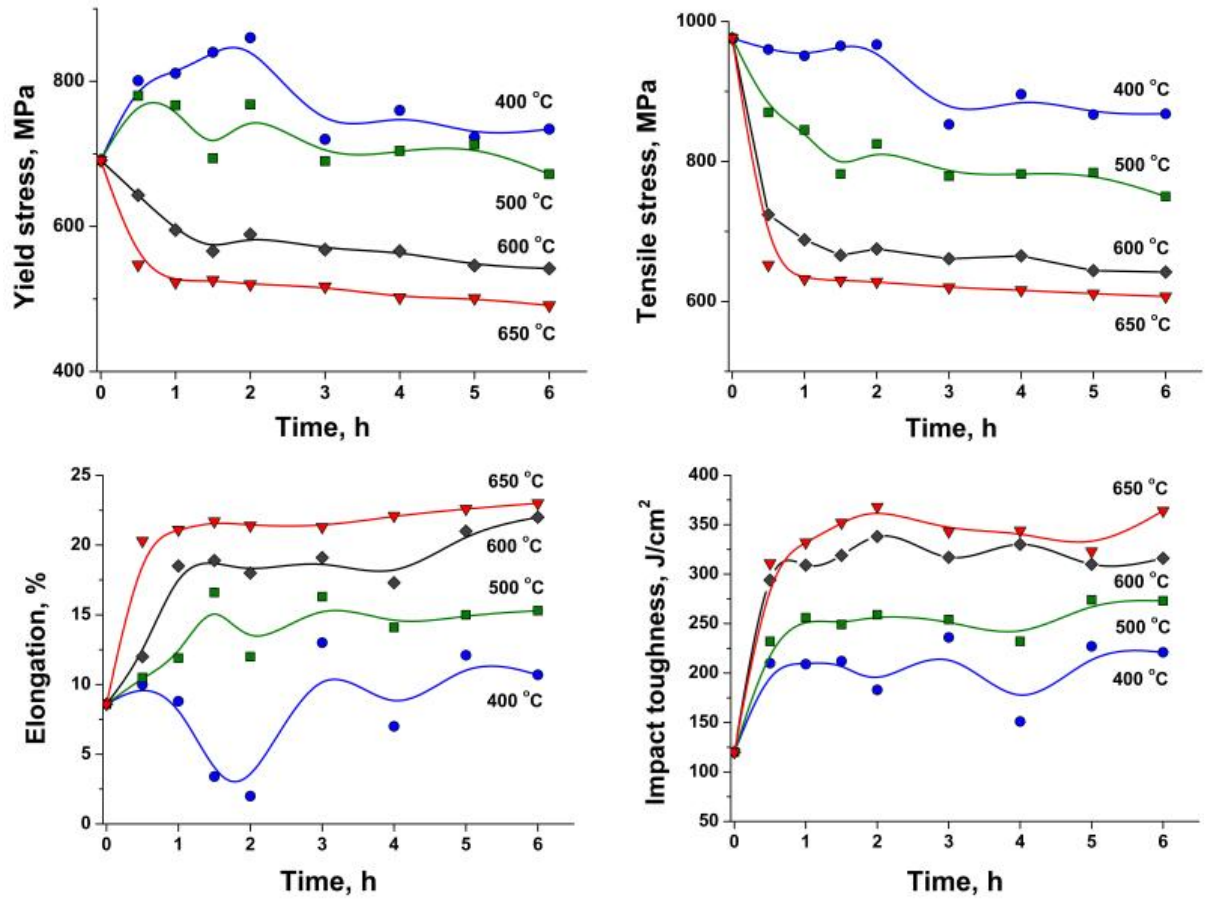
Yield stress, MPa
Time, h
400 °C
500 °C
600 °C
650 °C
Tensile stress, MPa
Time, h
Elongation, %
Time, h
Impact toughness, J/cm²
Time, h

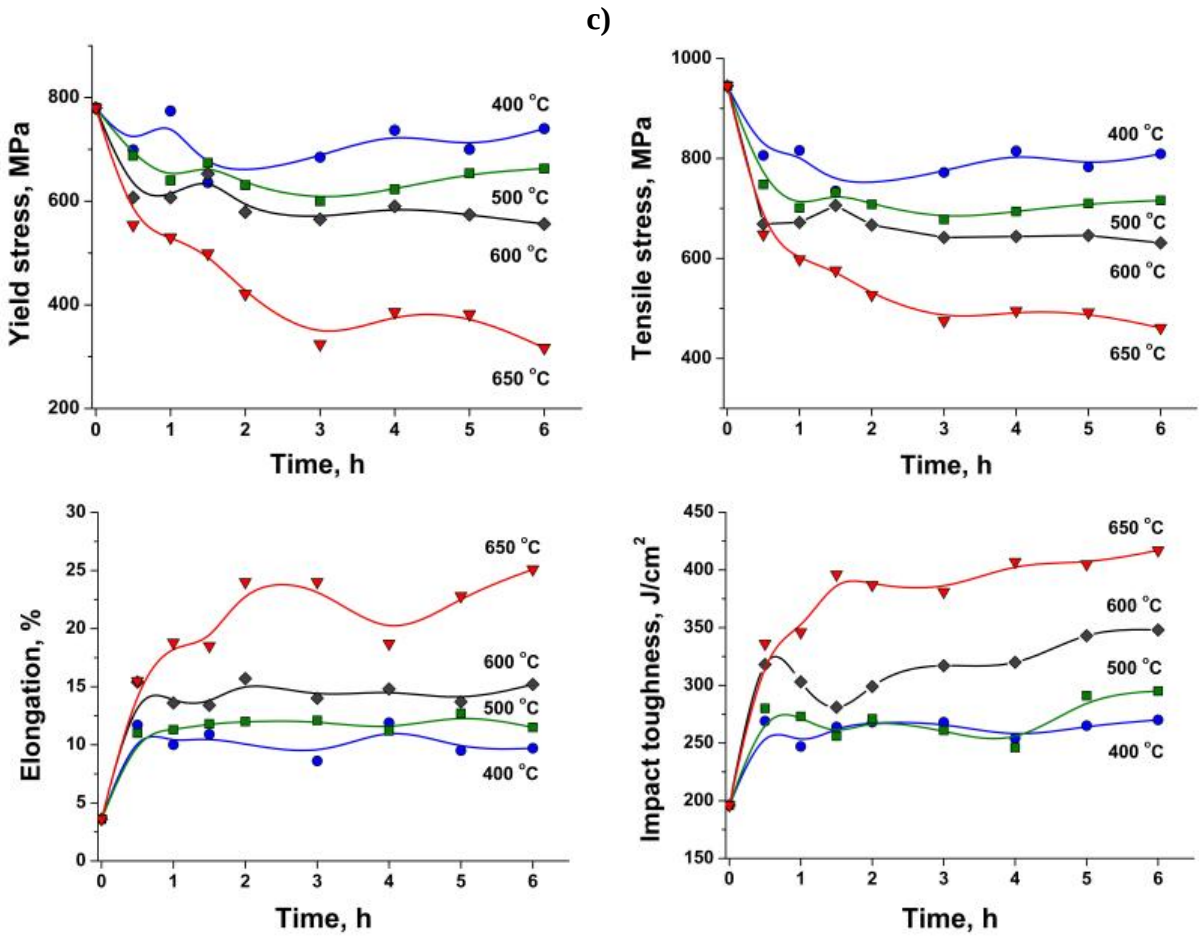

Fig. 2. Time dependences of yield stress, ultimate tensile stress, relative elongation (δ_5), and impact toughness (KCV) at various tempering temperatures for steels S1(a), S5(b), S7(c)

Figure 2 illustrates a complex evolution of steel properties in the tempering; it is particularly notable for the relative elongation and impact toughness of some steels (e.g. S5, S7). This behaviour is due to a complicated interdependence of the recovery and processes of precipitation/dissolution of various particle types (cementite, carbides of chromium, vanadium, and molybdenum as well as copper particles). The obtained data are used in the calibration of models for mechanistic properties as follows.

3. Description of the models, calibration procedure, and modeling results

The models for mechanical properties (yield stress (σ_Y), tensile stress (σ_T), relative elongation ($\delta \equiv \delta_5$)) are based on the mixture rule relating the contributions of individual structural components to their volume fractions. The following structural components are considered: polygonal ferrite (PF), bainite (B) of different morphology (granular (GB), lath (LB)), and martensite (M). Mechanical properties are estimated using the equations

$$\begin{aligned}
\sigma_Y &= \sigma_0^Y + \Delta\sigma_{ss}^Y + \Delta\sigma_{PF}^Y + \Delta\sigma_B^Y + \Delta\sigma_M^Y, \\
\sigma_T &= \sigma_0^T + \Delta\sigma_{ss}^T + \Delta\sigma_{PF}^Y + \Delta\sigma_B^T + \Delta\sigma_M^T, \\
\delta &= \delta_0 + \Delta\delta_{ss} + \Delta\delta_{PF} + \Delta\delta_B + \Delta\delta_M,
\end{aligned} \qquad (1)$$

where $\sigma_0^Y, \sigma_0^T, \delta_0$ are the base contributions; $\Delta\sigma_{ss}^Y, \Delta\sigma_{ss}^T, \Delta\delta_{ss}$ are the solid solution contributions; $\Delta\sigma_{SC}^Y, \Delta\sigma_{SC}^T, \Delta\delta_{SC}$ are contributions of the corresponding structural components (SC = PF, GB, LB, M) where the base and solid solution effects are excluded.

When evaluating respective effects on the relative elongation, it is supposed that each contribution to the hardening specifically diminishes the elongation.

To determine the hardening effect of solid solution, the following expressions are used

$$\Delta\sigma_{ss}^{Y;T} = \sum_{X} \alpha_{ss,X}^{Y;T} w_X ,$$
$$\Delta\delta_{ss} = -\alpha_{ss_0}^{E} \left(\sum_{X} \alpha_{ss,X}^{E} w_X \right)^{\beta_{ss}^{E}} , \quad (2)$$

where w_X is the dissolved content of alloying element X (mass.%); $\alpha_{ss,X}^{Y;T}$, α_{ss0}^{E}, $\alpha_{ss,X}^{E}$, β_{ss}^{E} are empirical model parameters.

According to the obtained metallographic data (Fig. 1), the considered steel structures have an insignificant quantity of polygonal ferrite. This conclusion complies with the estimate with AusEvol Pro predicting in steels the ferrite fraction that does not exceed 8% (Table 2). Nonetheless, the present model allows for the related small effects which are evaluated by

$$\Delta\sigma_{PF}^{Y;T} = \left(\Delta\sigma_{PF_{gb}}^{Y;T} + \Delta\sigma_{PF_{ppt}}^{Y;T} \right) X_{PF} ,$$
$$\Delta\delta_{PF} = -\left(\Delta\delta_{PF_{gb}}^{E} + \Delta\delta_{PF_{ppt}}^{E} \right) X_{PF} , \quad (3)$$

where $\Delta\sigma_{PF_{gb}}^{Y;T}$, $\Delta\delta_{PF_{gb}}^{E}$ are the ferrite grain boundaries contributions; $\Delta\sigma_{PF_{ppt}}^{Y;T}$, $\Delta\delta_{PF_{ppt}}^{E}$ are the contributions caused by carbonitrides/carbides particles (Nb(C,N), V(C,N), TiC) formed in austenite at the stage of hot rolling and inherited by the polygonal ferrite, as well as other components of the structure, after the corresponding transformation; X_{PF} is the polygonal ferrite volume fraction. Ferrite grain boundaries contributions are calculated according to the Hall-Petch equation

$$\Delta\sigma_{PF_{gb}}^{Y;T} = \alpha_{gb}^{Y;T} d_{PF}^{-0.5} ,$$
$$\Delta\delta_{PF_{gb}}^{E} = -\alpha_{gb}^{E} d_{PF}^{0.5} , \quad (4)$$

where d_{PF} is an average volumetric ferrite grain size (mm); $\alpha_{gb}^{Y;T}$, α_{gb}^{E} are empirical model parameters. Contributions of particles will be further considered.

The bainite contributions are expressed by equations

$$\Delta\sigma_{B}^{Y;T} = \sum_{k} \left(\Delta\sigma_{B_{0},k}^{Y;T} + \Delta\sigma_{B_{d},k}^{Y;T} + \Delta\sigma_{B_{ppt}}^{Y;T} \right) X_{B,k} ,$$
$$\Delta\delta_{B} = -\sum_{k} \left(\Delta\delta_{B_{0},k} + \Delta\delta_{B_{d},k} + \Delta\delta_{B_{ppt}}^{E} \right) X_{B,k} , \quad (5)$$

where $X_{B,k}$ is the volume fraction of k-th constituent in the bainite structure (k = GB, LB); $\Delta\sigma_{B_0,k}^{Y;T}$, $\Delta\delta_{B_0,k}$ are empiric parameters reflecting effects specific for various morphological types of bainite; $\Delta\sigma_{B_d,k}^{Y;T}$, $\Delta\delta_{B_d,k}$ dislocation contributions; $\Delta\sigma_{B_{ppt}}^{Y;T}$, $\Delta\delta_{B_{ppt}}^{E}$ are contributions of particles precipitated in bainite. These particles include both carbonitride/carbides preformed in austenite (Nb(C,N), V(C,N), TiC) and particles that appeared in bainite during the tempering (Fe_3C, V_4C_3, Mo_2C, Cr_7C_3, Cu).

Dislocation contributions are evaluated by expressions

$$\Delta\sigma_{B_d,k}^{Y;T} = \alpha_{B_d,k}^{Y;T} G_\alpha b \rho_{B_d,k}^{0.5} ,$$
$$\Delta\delta_{B_d,k} = -\alpha_{B_d,k}^{E} G_\alpha b \rho_{B_d,k}^{0.5} , \quad (6)$$

where $\rho_{B_d,k}$ is the average dislocation density in bainite of k-th type; $G_\alpha = 8.1\times10^{4}$ MPa is the shear modulus of the α-phase; $b = 2.5\times10^{-10}$ m is the Burgers vector magnitude;

$\alpha^{Y;T}_{B_d,k}$, $\alpha^{E}_{B_d,k}$ are empirical model parameters. Average dislocation densities for different morphologies of bainite and martensite are calculated with the formula [8]

$$\log_{10}(\rho_d, m^{-2}) = 9.2848 + \frac{6880}{\tilde{T}} - \frac{1780360}{\tilde{T}^2}, \tag{7}$$

where ρ_d is the dislocation density in the corresponding structural component formed at average temperature $\tilde{T}$ (K). Accordingly, the average dislocation density in the k-th type of bainite $\rho_{B_d,k}$ is calculated with Eq. (7) in which it is assumed that $\tilde{T} = \tilde{T}_{B,k}$.

Martensite contributions are determined in a similar way

$$\begin{aligned} \Delta\sigma^{Y;T}_{M} &= \left(\Delta\sigma^{Y;T}_{M_0} + \alpha^{Y;T}_{M_d} G_\alpha b \rho^{0.5}_{M_d} + \Delta\sigma^{Y;T}_{M_{ppt}}\right) X_M, \\ \Delta\delta_{M} &= -\left(\Delta\delta_{M_0} + \alpha^{E}_{M_d} G_\alpha b \rho^{0.5}_{M_d} + \Delta\delta^{E}_{M_{ppt}}\right) X_M, \end{aligned} \tag{8}$$

where X_M is the volume fraction of martensite; ρ_{M_d} is the average dislocation density in martensite calculated with Eq. (7) at the average temperature of its formation $\tilde{T} = \tilde{T}_M(K)$; $\Delta\sigma^{Y;T}_{M_{ppt}}$, $\Delta\delta^{E}_{M_{ppt}}$ are contributions of particles of the same types as in case of bainite; $\Delta\sigma^{Y;T}_{M_0}$, $\alpha^{Y;T}_{M_d}, \Delta\delta_{M_0}, \alpha^{E}_{M_d}$ are empirical parameters of the model.

To allow for the effects of particles on the yield stress of the considered microstructural constituents, it is presumed that moving dislocations overcome such barriers by means of bowing. Accordingly, the contribution of i-th particles type to yield stresses of all structural components takes on the form [9]

$$\begin{aligned} \Delta\sigma^{Y}_{ppt,i} &= \frac{\alpha^{Y}_{ppt} G_\alpha b}{\lambda_{ppt,i} - \bar{D}_{ppt,i}} \ln\left(\frac{\bar{D}_{ppt,i}}{1.5b}\right), \\ \lambda_{ppt,i} &\simeq 0.6\sqrt{\frac{2\pi}{3f_{ppt,i}}}\bar{D}_{ppt,i}, \end{aligned} \tag{9}$$

where $\bar{D}_{ppt,i}$, $f_{ppt,i}$ are the average diameter and volume fraction, respectively, for i-th type of particles (i= 1, 2, …, 8 respectively correspond to Nb(C,N), V(C,N), TiC, Fe_3C, V_4C_3, Mo_2C, Cr_7C_3, Cu); $\lambda_{ppt,i}$ is the average spacing of particle centers in slip planes of dislocations; α^{Y}_{ppt} (~ 0.1) is an empirical parameter.

The Pythagorean superposition rule [10] was employed to calculate contributions of all particles to mechanical properties of various structural constituents while presuming similar effects of the particles in bainite and martensite

$$\Delta\sigma^{Y}_{PF_{ppt}} = \sqrt{\sum_{i=1}^{3}(\Delta\sigma^{Y}_{ppt,i})^2},$$

PF:
$$\begin{aligned} \Delta\sigma^{T}_{PF_{ppt}} &= \sqrt{\sum_{i=1}^{3}(\alpha^{T}_{ppt,i}\Delta\sigma^{Y}_{ppt,i})^2}, \\ \Delta\delta^{E}_{PF_{ppt}} &= -\sqrt{\sum_{i=1}^{3}(\alpha^{E}_{ppt,i}\Delta\sigma^{Y}_{ppt,i})^2}, \end{aligned} \tag{10}$$

B, M:
$$\Delta\sigma^{Y}_{B;M_{ppt}} = \sqrt{\sum_{i=1}^{8}(\Delta\sigma^{Y}_{ppt,i})^2}, \tag{11}$$

$$\Delta\sigma^{T}_{B;M_{ppt}} = \sqrt{\sum_{i=1}^{8}(\alpha^{T}_{ppt,i}\Delta\sigma^{Y}_{ppt,i})^2}\,,$$

$$\Delta\delta^{E}_{B;M_{ppt}} = -\sqrt{\sum_{i=1}^{8}(\alpha^{E}_{ppt,i}\Delta\sigma^{Y}_{ppt,i})^2}\,,$$

in these expressions $\alpha^{T}_{ppt,i}$, $\alpha^{E}_{ppt,i}$ are empirical coefficients.

All empirical parameters employed in the prediction of mechanical properties of steel after its quenching and following tempering have been fitted to experimental results obtained in the present work. These data cover a wide range of chemical compositions (10 steels represented in Table 1) and various tempering temperatures and durations. Additionally, by means of the AusEvol Pro software, the involved microstructural characteristics have been derived from known industrial modes of hot rolling and conditions of the subsequent cooling. These characteristics include volume fractions of structural constituents, dimensions of ferrite grains, dislocation densities in bainite and martensite, volume fractions and average sizes of precipitated particles, dissolved quantities of alloying elements. To simulate the microstructure evolution including all considered particle types with allowance for both the recovery and precipitation phenomena, the current version of AusEvol Pro makes use of the authors' model [5].

Table 3. Parameters determining the contributions to hardening of bainite and martensite

Bainite					
$\Delta\sigma^{Y}_{B_0,GB}$, MPa	$\Delta\sigma^{T}_{B_0,GB}$, MPa	$\Delta\delta_{B_0,GB}$, %	$\Delta\sigma^{Y}_{B_0,LB}$, MPa	$\Delta\sigma^{T}_{B_0,LB}$, MPa	$\Delta\delta_{B_0,LB}$, %
160	120	10	165	130	8
$\alpha^{Y}_{B_d,GB}$, -	$\alpha^{T}_{B_d,GB}$, -	$\alpha^{E}_{B_d,GB}$, %/MPa	$\alpha^{Y}_{B_d,LB}$, -	$\alpha^{T}_{B_d,LB}$, -	$\alpha^{E}_{B_d,LB}$, %/MPa
0.48	0.55	7.0×10^{-3}	0.83	0.74	20.0×10^{-3}
Martensite					
$\Delta\sigma^{Y}_{M_0}$, MPa	$\Delta\sigma^{T}_{M_0}$, MPa	$\Delta\delta_{M_0}$, %	$\alpha^{Y}_{M_d}$, -	$\alpha^{T}_{M_d}$, -	$\Delta\delta_{M_d}$, %/MPa
125	115	9	0.84	0.83	9.0×10^{-3}

The model calibration leads to $\Delta\sigma^{Y}_{0}=103$ MPa, $\Delta\sigma^{T}_{0}=145$ MPa, $\Delta\delta_{0}=48\,\%$ for the base contribution to mechanical properties. When evaluating parameters to express solid solution effects (Eq. (2)), the authors used published approaches [11] as well as their own expressions [12]. These relationships were refined in what concerns the effects of Mn, Si, Mo, and N atoms. Respective results take on the form

$$\begin{aligned}
\Delta\sigma^{Y}_{ss} &= 52w_{Mn}+61w_{Si}+15w_{Ni}+39w_{Cu}+85w_{Mo}+42w_{Cr}+80w_{Ti}+678w_{P}+4000w^{free}_{N}\,,\\
\Delta\sigma^{T}_{ss} &= 58w_{Mn}+110w_{Si}+15w_{Ni}+39w_{Cu}+55w_{Mo}+30w_{Cr}+80w_{Ti}+678w_{P}+3400w^{free}_{N}\,,\\
\Delta\delta_{ss} &= -0.8\left(\begin{matrix}61w_{Mn}+50w_{Si}+15w_{Ni}+39w_{Cu}+11w_{Mo}+84w_{Cr}+80w_{Ti}+\\ +678w_{P}+5000w^{free}_{N}\end{matrix}\right)^{0.5}\,,
\end{aligned} \qquad (12)$$

where w_N^{free} is the quantity of free nitrogen avoiding capture by TiN, Nb(C,N), and V(C,N) particles.

To evaluate the effects of the ferrite grain boundaries, the following parameters were used: $\alpha_{gb}^{Y} = 18.3\ \text{MPa} \times \text{mm}^{0.5}$; $\alpha_{gb}^{T} = 17.2\ \text{MPa} \times \text{mm}^{0.5}$; $\alpha_{gb}^{E} = 1.9\ \% \times \text{mm}^{-0.5}$.

Except for contributions of precipitated particles, parameters determining contributions of bainite and martensite are listed in Table 3.

To substitute in Eq. (9), $\alpha_{ppt}^{Y} = 0.43$ has been found. Other parameters determining the particle contributions are represented in Table 4.

Table 4. Parameters determining contributions to hardening of various particles

Particle type	1 Nb(C,N)	2 V(C,N)	3 TiC	4 Fe_3C	5 V_4C_3	6 Mo_2C	7 Cr_7C_3	8 Cu
$\alpha_{ppt,i}^{T}$	0.41	0.37	0.32	0.37	0.64	0.35	0.28	0.43
$\alpha_{ppt,i}^{E}$	0.043	0.039	0.032	0.013	0.021	0.004	0.014	0.017

The comparison of predicted and measured mechanical properties shown in Fig. 3 demonstrates the reasonable performance of the model.

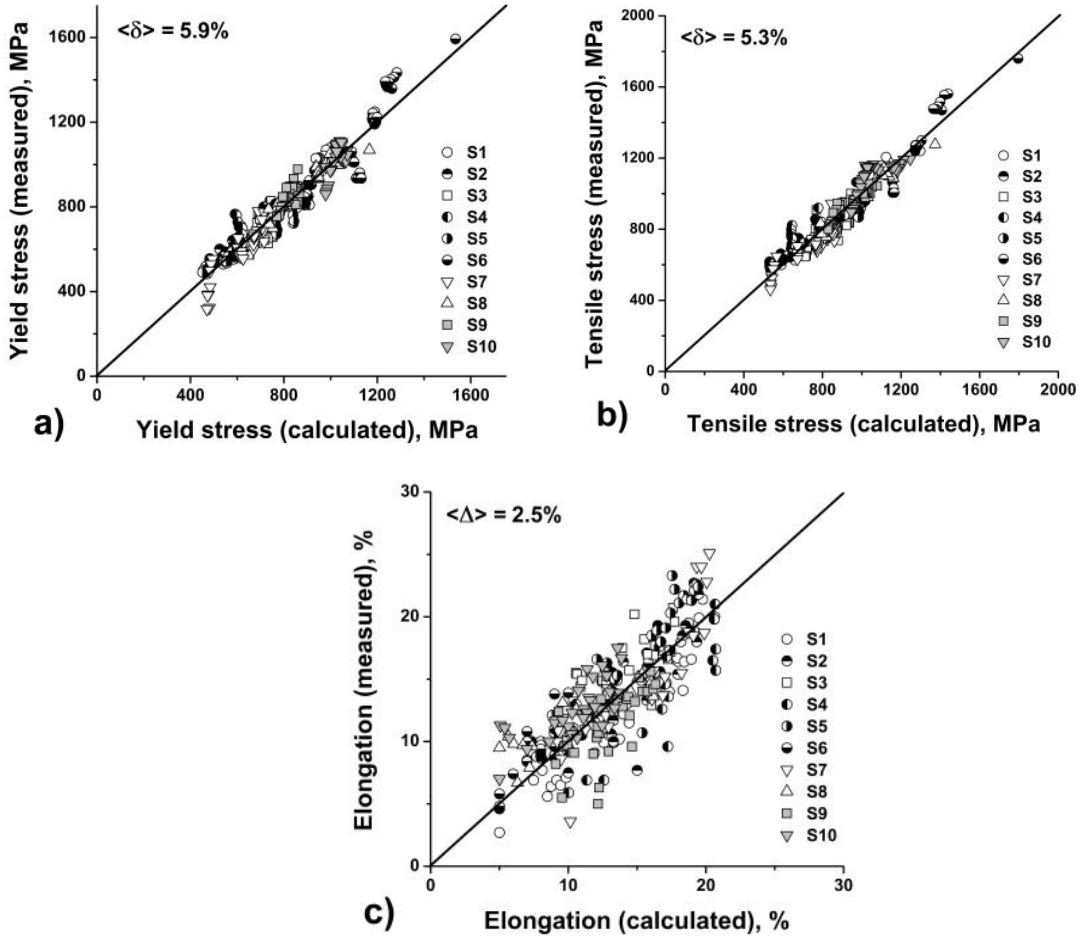

Fig. 3. Comparison of the calculated and measured mechanical properties of the investigated steels.
a) yield stress; b) tensile stress; c) relative elongation (δ_5).
<δ> and <Δ> are values of the average relative and absolute errors

4. Conclusions

Dependences of mechanical properties and the impact toughness on the tempering time at various temperatures have been experimentally investigated for 10 industrial bainitic-martensitic steels with a wide range of chemical compositions. Based on the obtained results, a model has been developed that predicts the mechanical properties of these steels after their quenching and the following tempering. In addition to the experimental results, microstructural parameters derived with the AusEvol Pro software from the given hot rolling modes and conditions of cooling are employed to calibrate the model. The modeling results comply well with experiments.

References

[1] Rybin VV, Malyshevsky VA, Oleinik VN, Sosenushkin EM, Sherokhina LG. Structural transformations during secondary hardening of low-carbon alloyed steels. *Metal Physics and Metallography*. 1976;41(4): 796-804. (In Russian)

[2] Ustinovshchikov YI, Kovensky IM, Vlasov VA. Mechanism of formation of special carbides in steels alloyed with chromium, molybdenum or vanadium. *Metal Physics and Metallography*. 1976;41(1): 99-111. (In Russian)

[3] Yamasaki S, Bhadeshia HKDH. Modelling and characterization of V_4C_3 precipitation and cementite dissolution during tempering of Fe–C–V martensitic steel. *Materials Science and Technology*. 2003;19: 1335-1343.

[4] Yamasaki S. *Modelling Precipitation of Carbides in Martensitic Steels. PhD Thesis.* University of Cambridge; 2004.

[5] Vasilyev AA, Sokolov SF, Sokolov DF. Modeling of carbides and copper particles precipitation during tempering of bainitic-martensitic Cr-Mo-V-Cu steels. *Materials Physics and Mechanics*. 2021;47(4): 543-556.

[6] Vasilyev AA, Sokolov DF, Sokolov SF. Modeling microstructure evolution during thermomechanical processing and heat treatment of steels and predicting their mechanical properties. *Materials Physics and Mechanics*. 2020;45(1): 8-19.

[7] Vasilyev AA, Sokolov DF, Sokolov SF, Kolbasnikov NG. Integral computer model for simulating microstructure evolution during thermomechanical processing and heat treatment of steels and predicting their final mechanical properties. *Materials Science Forum*. 2021;1016: 1532-1537.

[8] Bhadeshia HKDH. *Bainite in Steels: Transformations, Microstructure and Properties*. London: IOM Communications; 2001.

[9] Martin JW. *Micromechanisms in Particle-Hardened Alloys*. London: Cambridge University Press; 1980.

[10] Koppenaal TJ, Kuhlmann-Wilsdorf D. The effect of prestrassing on the strength of neutron-irradiated copper single crystals. *Applied Physics Letters*. 1964;4(3): 59-63.

[11] Gladman E. *The Physical Metallurgy of Microalloyed Steels*. London: The Institute of Materials; 1997.

[12] Sokolov D, Vasilyev A, Ogoltcov A, Sokolov S, Kolbasnikov N. Modeling mechanical properties of steels with complex microstructure. In: *METAL 2014 Conference Proceedings*. 2014. p.482-487.

THE AUTHORS

Vasilyev A.A.
e-mail: vasilyev_aa@mail.ru
ORCID: 0000-0002-5094-5104

Sokolov D.F.
e-mail: sklv.d.f@gmail.com
ORCID: 0000-0002-7661-6296

Sokolov S.F.
e-mail: sok_s_w@mail.ru
ORCID: 0000-0002-8139-8270